Sonochemical Synthesis, Thermal Studies and X-ray Structure of Precursor $[Zr(acac)_3(H_2O)_2]Cl$ for Deposition of Thin Film of ZrO_2 by Ultrasonic Aerosol Assisted Chemical Vapour Deposition

Muzammil Hussain, Muhammad Mazhar,* Muhammad Khawar Rauf,† Masahiro Ebihara,‡ and Tajammal Hussain‡

Department of Chemistry, ‡National Centre of Physics, Quaid-i-Azam University, Islamabad-45320, Pakistan
**E-mail: mazhar42pk@yahoo.com*
†Department of Chemistry, Faculty of Engineering, Gifu University, Yanagido, Gifu 501-1193, Japan
Received June 23, 2008, Accepted October 20, 2008

A new precursor $[Zr(acac)_3(H_2O)_2]Cl$ was synthesized by Sonochemical technique and used to deposit thin ZrO_2 film on quartz and ceramic substrate via ultrasonic aerosol assisted chemical vapour deposition (UAACVD) at 300 °C in oxygen environment followed by annealing of the sample for 2-3 minutes at 500 °C in nitrogen ambient. The molecular structure of the precursor determined by single crystal X-ray analysis revealed that the molecules are linked through intermolecular hydrogen bonds forming pseudo six and eight membered rings. DSC and TGA/FTIR techniques were used to determine thermal behavior and decomposition temperature of the precursor and nature of evolved gas products. The optical measurement of annealed ZrO_2 film with tetragonal phase shows optical energy band gap of 5.01 eV. The particle size, morphology, surface structure and composition of deposited films were investigated by XRD, SEM and EDX.

Key Word : Zirconium oxide, Thin film, Energy band gap, SEM, Single crystal X-ray analysis

Introduction

Over the past three decades most of the scientific and engineering research has been conducted in the field of ceramic coating technology because of their good thermal, mechanical and chemical stability. Among many transition metal oxides such as ZrO_2, HfO_2[1] and La_2O_3,[2-5] ZrO_2 having high dielectric constant have been considered an alternative gate dielectric, because of their thermodynamic stability in contact with silicon.[6] Moreover ZrO_2 film has found use in coating technology because of its high strength, fracture toughness, low chemical inertness, thermal stability, high refractive index and low optical absorption.[7,8]

One interesting property of ZrO_2 is that it is polymorphic in nature and possesses several crystal structures at different temperatures that allow its grain size control and opportunity to tune its specific properties for a specific application.[9]

Several coating technologies like sol gel,[10] electron beam evaporation,[11] CVD[12] and especially MOCVD[13] were used for thin film deposition, however, films deposited by these have shown micro cracks, and voids which degrade the quality of thin film.

A variety of precursors such as $ZrCl_4$,[14-17] ZrI_4,[18,19] $Zr(OBu)_4$,[20] $Zr(thd)_4$,[21] $Zr(OBu)(dmae)_2$[22] have been used in the past but suitability of the alkoxide limits application of the precursors. Zirconium oxychloride octahydrate ($ZrOCl_2 \cdot 8H_2O$) has been also used in fabrication of thin film of zirconium oxide (ZrO_2) using a sol-gel method but the method needs extra care, greater process time and high cost. This process starts from immersion of the substrate into the solution, followed by drying and baking in a furnace with a temperature above 300°C. Deterioration of the solution with time is also another problem. Similarly Yanfeng Gao have also prepared ZrO_2 thin film using self-assembled mono layer technique (SAM) by the controlled hydrolysis of $ZrOCl_2 \cdot 8H_2O$ in ethanol at 50°C, however, a large amount of chlorine was present in the as-deposited thin film because of partial hydrolysis of zirconium ethoxide.[23,24] It has been reported[25] that β-diketonates and their derivatives are more stable and readily soluble in organic solvent than alkoxides and can be used successfully for ceramic thin film deposition.[26-29]

Keeping all these difficulties in view, we adopted a sonochemical method for the synthesis of precursor $[Zr(acac)_3(H_2O)_2]Cl$, which seems to have advantage over $ZrCl_2[(SiMe_3)_2]_2$ and zirconium alkanides.[30] In the past years sonochemical synthetic technique has largely been applied to organic synthesis and little attention was paid to synthesize inorganic materials for commercial utility. It is also observed that metal halides and metal acetylacetonate react with alkali metals sonochemically and give reactive metal (M^+) that reacts instantly with organic ligands to yield respective metal organic complexes. For instance, Ni^+ produced from reaction of nickel acetylacetonate and sodium metal, reacts in situ with 1,5 cyclopentadiene (COD) to yield $Ni(COD)_2$.[31] Similarly in conventional synthesis procedure, metal carbonyl complexes are accessible from transition metal halides, sodium and carbon monoxide, but this reaction requires temperature of 100-300°C under high pressure, even when using freshly prepared Rieke's metals. The use of sonochemistry facilitate the reduction steps to yield the required product under mild conditions.[32]

In continuation with our previous studies,[33] we report here a quick and high yield sonochemical method for the synthesis of low melting precursor $[Zr(acac)_3(H_2O)_2]Cl$ for the deposition of ZrO_2 thin film by ultrasonic aerosol assisted chemical vapour deposition technique.

Materials and Instrumentation

Analytical grade reagents purchased from E.Merck were used for the synthesis of the precursor without any further puri-

fication and all experiments were performed in air ambient. All syntheses were performed under ultrasonic irradiation using a 20 KHz ultrasonic generator. Melting point was measured with a GallenKamp 3A-3790 apparatus. CHNO and Zn analysis was performed using a CHNS-O Flash EA 1112 analyzer of Thermoelectron and an Atomic Absorption Analyzer (GBC). Thermal studies and decomposition patterns were studied using a DSC 823^e and TGA/SDAT 851^e from Mettler Toledo coupled with an FTIR Nexus 470 of Thermo Nicolet. The crystals of $[Zr(acac)_3(H_2O)_2]Cl$ were grown by slow evaporation of 2-methoxy ethanol/acetonitrile (1:1) solution at room temperature. The reflection data for the colorless crystal mounted on a glass fiber were collected with a Rigaku AFC7R Mercury CCD diffractometer with graphite monochromated MoKα radiation (λ = 0.71069Å). The structure was solved by using direct methods, Sir97[34] and refined by Shelxl97.[35] All the non-hydrogen atoms were refined anisotropically. The H atoms attached to oxygen were refined isotropically. Other hydrogen atoms were located at the calculated positions and refined as riding atoms. Table 2. summarizes the crystal data and refinement description.Film thicknesses were measured using a sigma scan analyzer (Stylo, USA). Powder X-ray diffraction studies were performed using a PAN Analytical X' Pert PRO diffractometer equipped with a Cu source (Cu K_α, λ = 1.5405 Å). Peak intensities, d- spacing, 2θ values and integral breadth of the reflections were determined with X'Pert Data Collector software. SEM and EDX (JOEL-JSM-5910) were used to observe surface morphology, average particle size and composition of the deposited material. The optical transmittance of the ZrO_2 films was determined using a UV-Vis spectrophotometer (MPC-3100, Schimadzu).

Synthesis of $[Zr(acac)_3(H_2O)_2]Cl$. 3.0 g (0.01 mmol) $ZrOCl_2 \cdot 8H_2O$ and 6 g (0.06 mmol) of acetylacetone, 10 ml of 2-methoxy ethanol were added in 250 ml Erlenmeyer flask to give turbid solution. To this suspension 10ml of acetonitrile was added and the solution was irradiated in an ultrasonic generator for about half an hour to yield clear solution. The contents were set aside for 2 weeks to give off white block type crystals. The crystalline product was purified by washing with dry diethyl ether to yield 80% of the product (m.p. 98 °C). The CHNO and Zr analysis % found (calculated) for $ZrO_8C_{15}H_{25}Cl$ is C 39.34 (39.13), H 5.33 (5.43), O 27.98 (27.82), and Zr 19.89 (20.01).

FTIR absorption bands frequencies: 3400, 3068, 1571, 1528, 1430, 1384, 1351, 1282, 1184, 1023, 933, 831, 780, 752, 660, 538 cm^{-1}.

Thermal Study. Thermal behavior of $[Zr(acac)_3(H_2O)_2]Cl$ was studied in the range of 30-500 °C with a heating rate of 10 °C/min under an oxygen atmosphere in an open lid 70 μL alumina crucible using a Mettler Toledo DSC 823^e and TGA/SDTA 851^e instrument to determine the decomposition temperature. The purge gas and the evolved gases from the sample were transferred from the TGA to the FTIR through a transfer line that was kept constantly at 250 °C in order to avoid any condensation of the evolved gases. FTIR scans of the gases were taken at *ca.* every twenty seconds at a resolution of 4 cm^{-1}.

Thin Film Deposition. Apparatus used for deposition of thin film is described elsewhere in detail.[33] The conditions used for the growth of the ZrO_2 thin films are given in Table 1.

Table 1. Growth condition for the deposition of Zirconium oxide thin film from $[Zr(acac)_3(H_2O)_2]Cl$

Precursor concentration	150 mg/25 ml (methanol)
Carrier Gas (O_2) flow rate (cm^3/min)	25
Sample solution injection (ml/min)	0.5
Substrate	Quartz, Ceramic
Deposition time	10-30 min (depending on thickness)
Temperature of Substrate	300 °C

Table 2. Crystal data for $[Zr(acac)_3(H_2O)_2]Cl$.

Empirical formula	$ZrO_8C_{15}H_{25}Cl$
FW (amu)	460.02
Crystal system	triclinic
Space group	P -1
a (Å)	9.399 (3)
b (Å)	10.408 (3)
c (Å)	11.478 (3)
α (°)	70.182 (11)
β (°)	70.647 (10)
γ (°)	72.755 (10)
V (Å^3)	975.0(4)
Z	2
$d_{calcd.}$ (Mgm^{-3})	1.567
Absorption coefficient, μ(mm^{-1})	0.738
F(000)	475
θ range for data collection (o)	3.4 to 27.5
Reflection collected/ unique	7876/3617
Data/ restraints/ parameters	4415/0/249
Goodness-of-fit on F^2	1.061
Final R indicies [$I > 2\sigma(I)$]	R_1 = 0.0269, wR_2 = 0.0618
Largest diff. peak and hole (e Å^{-3})	0.414, -0.515

A solution of 150mg/25 ml in methanol was injected into Cole Palmer Ultrasonic Atomizer to generate the aerosol in an evacuated quartz chamber containing 50 × 40 mm gold coated ceramic wafers which were cleaned with deionized water, acetone and 1,1,1-trichloro ethane and then heated to 100 °C for twenty minutes before use. Oxygen gas and sample solution was injected through a control valve.

After half an hour, substrate was removed from the chamber and further annealed at 500 °C in ambient of nitrogen for 1-2 minutes to achieve the tetragonal crystalline structure. Crystallographic data for the structures reported here have been deposited with CCDC (Deposition No. CCDC-674643). These data can be obtained free of charge *via* http://www.ccdc.cam.ac.uk/conts/retrieving.html or from CCDC, 12 Union Road, Cambridge CB2 1EZ, UK, email: deposit@ccdc.cam.ac.uk.

Results and Discussion

$ZrOCl_2 \cdot 8H_2O$ dissolved in 2-methoxy ethanol/acetonitrile (1:1) mixture reacts quantitatively with acetylacetone (acacH) under ultrasonic irradiation for half an hour to give quantitative yield of the product $[Zr(acac)_3(H_2O)_2]Cl$ as shown in the following chemical equation. The product was purified by washing several times with dry diethylether.

$$ZrOCl_2{\cdot}8H_2O + 3C_5H_7O_2H \xrightarrow[\text{Acetonitrile:2-Methoxy ethanol}]{\text{Ultrasonic irradiation, 1/2 Hr}} [Zr(C_5H_7O_2)_3(H_2O)_2]Cl + 7H_2O + HCl$$

FTIR Studies. The most significant feature of the FTIR spectra of bis-aqua, tris-acetylacetonato zirconium (IV) chloride are recorded in the range of 4000-500 cm^{-1}. The presence of bands at 1528 cm^{-1} and 1571 cm^{-1} due to metal bonded C-O and at 1430 cm^{-1} and 1384 cm^{-1} due to C-C bond of acetylacetonate group.[9] In free acetylacetone two C-O bonds give a band pattern at 1600 cm^{-1} and 1500 cm^{-1} where as two C-C bonds give a band pattern at 1450 cm^{-1} and 1260 cm^{-1}. The lowering of absorption frequency of these two bonds indicates chelation of acetylacetone group to the metal center. A very broad peak at 3400-3068 cm^{-1} is assigned to water molecule present in the complex. Absorption peaks at 660 cm^{-1} and 538 cm^{-1} are due to M-Cl and M-O bond respectively. All these characteristic vibrational frequencies are found in good agreement with the proposed structure.

Single Crystal X-ray Analysis. The molecular structure of $[Zr(acac)_3(H_2O)_2]Cl$ is shown in Figure 1. The coordination environment of Zr atom in ZrO_8 moiety consist of three bidentate *O,O'*-chelating acetylacetonate and two monodentate water molecules. The ZrO_8 exhibits a distorted square-antiprism geometry. The average Zr-O distance 2.1819 Å and the bite angles O1-Zr1-O2, O3-Zr1-O4 and O5-Zr1-O6 are 75.75(5)°, 76.32(5)° and 75.57(5)° respectively are in good agreement with those reported for $Zr(acac)_4$.[10] Pairs of molecules are linked by O-H···O hydrogen bonds in cyclic dimmers, which are further packed into a three-dimensional framework by chains of O-H···Cl trifurcated hydrogen bonds. The Zr-O1 bond length is longer than the rest of Zr-O bonds, due to the elongation effect of hydrogen bonding. The overall lattice structure generated by the O-H···O and O-H···Cl hydrogen bonds is shown in Figure 2.

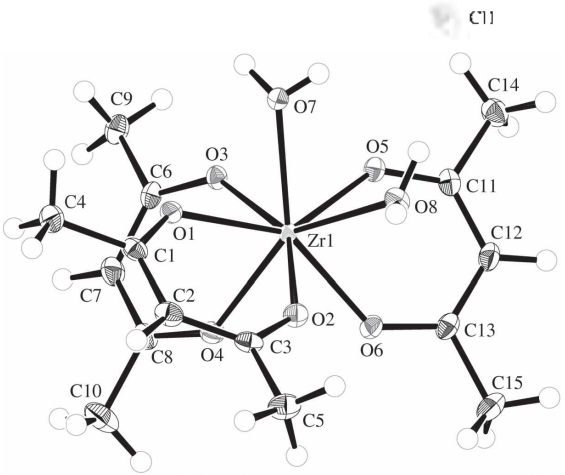

Figure 1. The asymmetric unit of $[Zr(acac)_3(H_2O)_2]Cl$ showing the labeling scheme used in the text and tables; atomic displacements are at the 30% level.

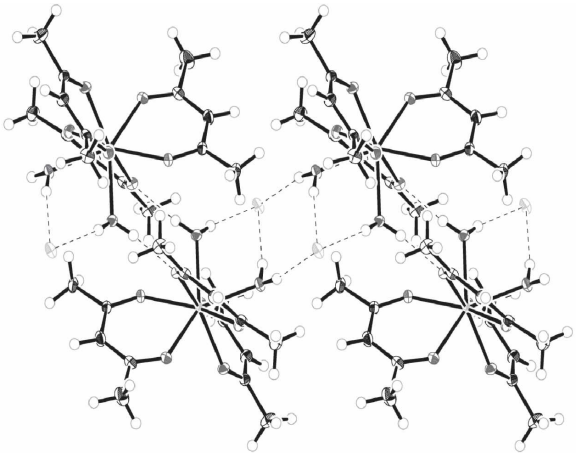

Figure 2. The lattice structure of $[Zr(acac)_3(H_2O)_2]Cl$ showing units linking through trifurcated chlorine atom and a network of H- bonds.

Thermal Studies. TGA, DTG and DSC curves for the decomposition of bis-aqua, tris-acetylacetonato zirconium (IV) chloride were recorded in an oxygen environment and are shown in Figure 3.

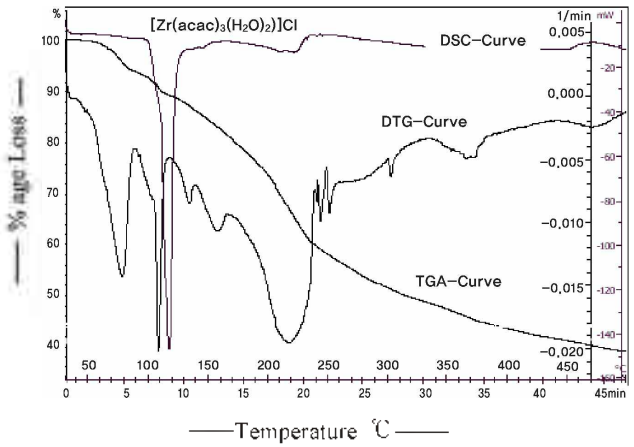

Figure 3. TGA/DTG/DSC curves showing the decomposition of $[Zr(acac)_3(H_2O)_2]Cl$.

Table 3. Selected bond lengths (Å) and angles (°) for $[Zr(acac)_3(H_2O)_2]Cl$

Bond lengths			
Zr(1)-O(6)	2.1370(13)	O(4)-Zr(1)-O(1)	77.69(5)
Zr(1)-O(3)	2.1424(13)	O(5)-Zr(1)-O(1)	140.96(5)
Zr(1)-O(2)	2.1506(13)	O(6)-Zr(1)-O(7)	144.22(5)
Zr(1)-O(4)	2.1597(13)	O(3)-Zr(1)-O(7)	75.24(5)
Zr(1)-O(5)	2.1808(13)	O(2)-Zr(1)-O(7)	113.21(5)
Zr(1)-O(1)	2.2336(12)	O(4)-Zr(1)-O(7)	139.93(5)
Zr(1)-O(7)	2.2756(14)	O(5)-Zr(1)-O(7)	75.45(5)
Zr(1)-O(8)	2.2756(14)	O(1)-Zr(1)-O(7)	70.11(5)
Bond angles		O(6)-Zr(1)-O(8)	80.98(5)
O(6)-Zr(1)-O(3)	115.60(5)	O(3)-Zr(1)-O(8)	138.21(5)
O(6)-Zr(1)-O(2)	75.79(5)	O(2)-Zr(1)-O(8)	69.52(5)
O(3)-Zr(1)-O(2)	149.17(5)	O(4)-Zr(1)-O(8)	144.67(5)
O(6)-Zr(1)-O(4)	74.46(5)	O(5)-Zr(1)-O(8)	74.21(5)
O(3)-Zr(1)-O(4)	76.32(5)	O(1)-Zr(1)-O(8)	110.24(5)
O(2)-Zr(1)-O(4)	79.98(5)	O(7)-Zr(1)-O(8)	71.28(5)
O(6)-Zr(1)-O(5)	75.57(5)	C(1)-O(1)-Zr(1)	133.86(11)
O(3)-Zr(1)-O(5)	73.74(5)	C(3)-O(2)-Zr(1)	138.17(12)
O(2)-Zr(1)-O(5)	136.51(5)	C(6)-O(3)-Zr(1)	136.39(11)
O(4)-Zr(1)-O(5)	121.98(5)	C(8)-O(4)-Zr(1)	134.35(12)
		C(11)-O(5)-Zr(1)	133.09(12)
O(6)-Zr(1)-O(1)	142.99(5)	C(13)-O(6)-Zr(1)	133.08(12)
O(3)-Zr(1)-O(1)	80.14(5)		
O(2)-Zr(1)-O(1)	75.75(5)		

The TG curve of the complex shows a gradual loss of weight of about 70 % around 450 °C to give a residual mass consisting of about 30 % close to that expected for a complete conversion to ZrO_2. DSC curve show that there is an initial endothermic behavior at about 125 °C and 230 °C followed by small exothermic peak between 250-300 °C. No significant weight loss was observed up to temperature of 90 °C. Initial stepwise weight loss up to 150 °C is associated with water and Cl (endothermic). The weight loss from 150 to 400 °C is linked with burning of acetylacetonate (exothermic) to acetone, CO_2 and H_2O.[37] There was no organic residue left after 450 °C as confirmed by the FTIR of residual mass.

SEM and EDX Studies. SEM and EDX investigated the morphology, surface structure and composition of the deposited films. The scanning electron microscopic image (Figure 4a) shows amorphous nature of deposited ZrO_2 particles as reported earlier.[38] The SEM micrograph (a) exhibits the uniformity of the film indicating no defect formation. However, a careful examination of SEM micrograph (Figure 4b) of the sample annealed at 500 °C shows emergence of defined grains. It has been reported that annealing of ZrO_2 causes loss of porosity, formation of new grains resulting a change in material properties.[39] The annealed films have a smooth uniform surface and densely polycrystalline microstructure with a particle size range of 40-50 nm. The elemental composition of annealed film as determined by EDX was found to be Zr, 25.2 at. %, O, 72.9 at. % and C 1.8 at. %.

XRD Studies. Figure 5 shows the XRD pattern of a ZrO_2 film recorded within an angle range of 15 to 80° for the as-deposited thin film (a) and that after annealing at 500 °C (b). The grain size of annealed thin film was determined using Debye-Scherrer equation.[40] peak intensities, d-spacing, 2θ values and integral breadth of the reflections were determined with X'Pert Data Collector software.

XRD patterns indicate that the ZrO_2 film structure depends strongly on annealing temperature. For as deposited film (Figure 5a) no diffraction peaks are observed which indicates amorphous nature of the film. This leads to a conclusion that this film is amorphous. Progressively with annealing at temperature 500 °C under N_2 atmosphere for 1-2 minutes, diffraction peak appearing at about 30.1, 34.2, 35.1 correspond to those from (101), (002) and (110) reflection planes respectively (JCPDS file 42-1164) indicating the crystallization of tetragonal ZrO_2 (Figure 5b). These results are in agreement with previous study.[30] It has been reported that at higher temperature the tetragonal phase change to new phase, monoclinic-ZrO_2, which was confirmed by decrease in intensity of (101) diffraction of tetragonal ZrO_2 and appearance of some new peaks (111, 011, 200, 020). The formation of metastable teteragonal ZrO_2 phase was preferred over monoclinic polymorph because of its stability even at temperature above 1000 °C and also due to its lower surface energy.[41] The average C-contents of thin film found to be around 7 atom % which drop to 1.8 atom % by annealing as estimated during EDX study.[42]

Optical Characterization. Optical characterization of the ZrO_2 thin film was carried out using UV-Vis spectrophotometer. A plot of absorbance vs wavelength in the wavelength range of 200-700 nm shown in Figure 6 indicates that the film is transparent and gives absorption edge at 235 nm as reported earlier.[9]

The optical band gap energy was calculated from the plot of $(\alpha.t.h\upsilon)^2$ $(eV)^2$ *vs.* hυ(eV) (Figure 7) for a film of thickness 500 nm, where α is absorption coefficient and was calculated from the transmission spectrum using equation $\alpha = \ln(1/T)/t$.[43] T is the transmittance and t is the thickness of the film. It can be seen that the plot is linear in the region of strong absorption edge indicating that the absorption takes place through direct transition. The optical band gap calculated from the plot was

Table 4. The intermolecular hydrogen bonds for $[Zr(acac)_3(H_2O)_2]Cl$

D	H	A	DH(Å)	HA(Å)	DA(Å)	DHA(°)
O7	H7A	O1	0.87(3)	1.90(3)	2.7678(19)	174(3)
O7	H7B	Cl1	0.79(3)	2.29(3)	3.0695(15)	171(3)
O8	H8A	Cl1	0.86(3)	2.25(3)	3.0967(16)	168(2)
O8	H8B	Cl1	0.90(3)	2.17(3)	3.0556(15)	167(3)

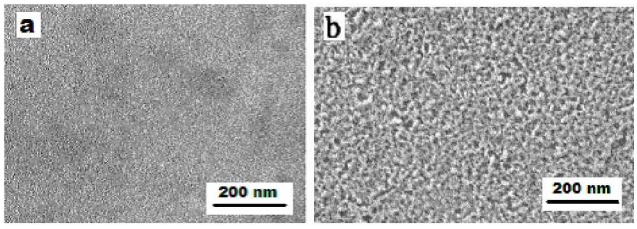

Figure 4. Comparison of SEM images of ZrO_2 thin film as deposited (a) and annealed (b).

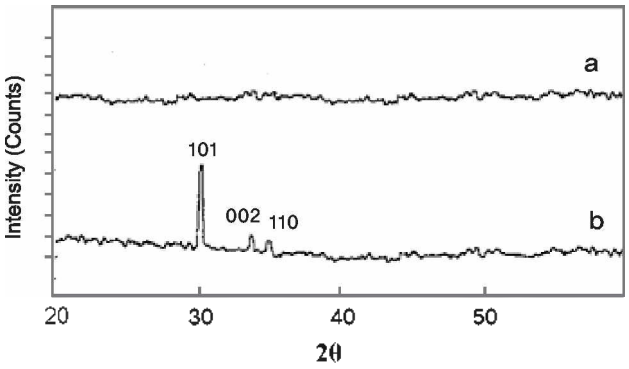

Figure 5. XRD patterns of ZrO_2 film deposited from $[Zr(acac)_3(H_2O)_2]Cl$ at (a) 300 °C, (b) annealed at 500 °C.

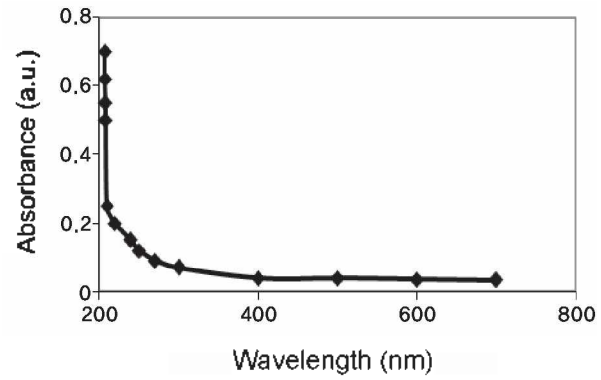

Figure 6. UV-Visible absorption spectrum of ZrO_2 thin film deposited on Quartz substrate.

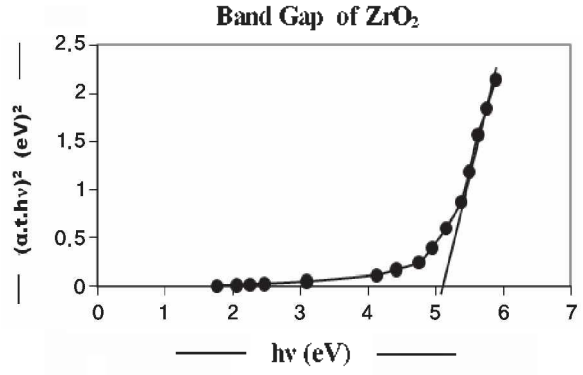

Figure 7. A plot of absorption coefficient (α^2) vs photon energy (hν) of ZrO_2 thin film.

found to be 5.01 eV, which is in agreement with the previous reported value for ZrO_2.[44]

Conclusion

A low melting highly volatile precursor $[Zr(acac)_3(H_2O)_2]Cl$ has been synthesized by sonochemical irradiation technique and used for growth of amorphous ZrO_2 thin films having particle size in the range of 40-50 nm by UAACVD. Annealing of the film at 500 °C in ambient of nitrogen gas produces tetragonal structured ZrO_2 with smooth surface morphology and optical bad gap of 5.01 eV.

Acknowledgments. MH and MM express their gratitude to the IICS technical staff for recording XRD data and Pakistan Science Foundation for financial support.

References

1. Kang, L.; Lee, B. H.; Qi, W. *IEEE Electron Device Lett.* **2000**, *76*, 112.
2. Guha, S.; Cartier, E.; Gribelyuk, M. A.; Borjarczuk, N. A.; Coppel, M. A. *Appl. Phys. Lett.* **2000**, *77*, 2710.
3. Wilk, G. D.; Wallace, R. M. *Appl. Phys. Lett.* **2000**, *76*, 112.
4. Wilk, G. D.; Wallace, R. M. *Appl. Phys. Lett.* **1999**, *74*, 2854.
5. Kim, W.; Kang, S.; Rhee, S.; Lee, N.; Lee, J.; Kang, H. *J. Vac. Sci. Technol. A* **2002**, *20*, 2096.
6. Qi, W.; Nieh, R.; Lee, B. H.; Kang, L.; Jeon, Y.; Onishi, K.; Ngai, T.; Banerjee, S.; Lee, J. C. *IEDM* **1999**, 145.
7. Bradley, D. C.; Thornton, P. *Comprehensive Inorganic Chemistry*; Trotman-Dichenson, A. F., Ed.; Pergamon Press: Oxford, 1973; Vol 3. p 426.
8. Apparao, K. V. S. R.; Sahoo, N. K.; Bagchi, T. C. *Thin Solid Films* **1985**, *L71*, 129.
9. Kim, D.-Y.; Lee, I.-H.; Park, S. J. *J. Mater. Res.* **1996**, *11*(10), 2583.
10. Brenier, R.; Mugnier, J.; Mirica, E. *Appl. Surf. Sci.* **1999**, *85*, 143.
11. Morita, M.; Fukumoto, H.; Imura, T.; Osaka, Y. *J. Appl. Phys.* **1985**, *56*, 2407.
12. Tauber, R. N.; Dumbri, A. C.; Caffrey, R. E. *J. Electrochem. Soc. Solid State Sci.* **1971**, *118*, 747.
13. Balog, M.; Schieber, M.; Michman, M.; Patai, S. *Thin Solid Films* **1977**, *47*, 109.
14. Ritala, M.; Leskela, M. *Appl. Surf. Sci.* **1994**, *75*, 333.
15. Kukli, K.; Thanaus, J.; Ritala, M.; Leskala, M. *J. Electrochem. Sci.* **1997**, *144*, 300.
16. Kukli, K.; Ritala, M.; Aarik, J.; Ustare, T.; Leskala, M. *J. Appl. Phys.* **2002**, *92*, 1833.
17. Cassir, M.; Goubin, F.; Bernay, C.; Vernoux, P.; Lincot, D. *Appl. Surf. Sci.* **2002**, *193*, 120.
18. Kukli, K.; Forsgren, K.; Aarik, J.; Ustare, T.; Aidla, A.; Niska, A.; Ritala, M.; Leskal, M.; Harsta, A. *J. Cryst. Growth* **2001**, 211, 300.
19. Kukli, K.; Ritala, M.; Ustare, T.; Aarik, J.; Forsgren, K.; Sajavaara, T.; Leskala, M.; Harsta, A. *Thin Solid Films* **2002**, *55*, 410.
20. Kukli, K.; Ritala, M.; Leskala, M. *Chem. Vap. Deposition* **2000**, *6*, 297.
21. Putknen, M.; Niinisto, L. *J. Mater. Chem.* **2001**, *11*, 3141.
22. Matero, R.; Ritala, M.; Leskela, M.; Jones, A. C.; William, P. A.; Bickley, J. F.; Steiner., A.; Leedham, T. J.; Davies, H. O. *J. Non-Cryst. Solids* **2002**, *24*, 303.
23. Gao, Y.; Masuda, Y.; Yonezawa, T.; Ohta, K.; Koumoto, K. *Chem. Mater.* **2004**, *16*, 2615.
24. Gao, Y.; Masuda, Y.; Yonezawa, T.; Koumoto, K. *J. Ceram. Soc. Jpn.* **2002**, *110*, 379.
25. Hugh, O. P. *Handbook of Chemical Vapour Deposition (CVD)*; Noyes Publications: New Jersey, U.S.A. 1999; p 91.
26. Balog, M.; Schieber, M.; Patai, S.; Michman, M. *Thin Solid Films* **1972**, *17*, 298.
27. Balog, M.; Schieber, M.; Michman, M.; Patai, S. *J. Cryst. Growth* **1972**, *47*, 109.
28. Putknen, M.; Niinisto, L. *J. Mater. Chem.* **2001**, *11*, 3141.
29. Matero, R.; Ritala, M.; Leskala, M.; Jones, A. C.; Williams, P. A.; Bickley, J. F.; Steiner, A.; Leedhan, T. J.; Davies, H. O. *J. Non-Cryst. Solids.* **2002**, *24*, 303.
30. Nam, W.-H.; Rhee, S.-W. *Chem. Vap. Deposition* **2004**, *10* (4), 201.
31. Han, B. H.; Boudjouk, P. *J. Org. Chem.* **1982**, *47*, 5030.
32. Lee, P. H.; Bang, K.; Lee, K.; Sung, S. Y.; Chang, S. *Syn. Commun.* **2001**, *31*, 3781.
33. Mazahar, M.; Hussain, S. M.; Faiz, R.; Gabricle, K.-K.; Kieran, C. M. *Bull. Korean Chem. Soc.* **2006**, *27*(10), 1573.
34. Altomare, A.; Burla, M. C.; Camalli, M.; Cascarano, G. L.; Giacovazzo, C.; Guagliardi, A.; Moliterni, A. G. G.; Polidori, G.; Spagna, R. *J. Appl. Crystallogr.* **1999**, *32*, 115.
35. Sheldrick, G. M. *SHELXL 9*; University of Gottingen, Germany, 1997.
36. Clegg, W. *Acta Cryst.* **1987**, *C43*, 790.
37. Hoene, J. Von.; Charles, R. G.; Hickam, W. M. *J. Phys. Chem.* **1958**, *62*, 1098.
38. Phale, P. R. *J. Mater. Res.* **1993**, *8*, 334.
39. Otsu, Y.; Egami, M.; Misawa, T.; Fujita, H.; Yukimura, K. *Paper of Technical Meeting on Electrical Discharge, IEE Japan* **2003**, *ED03*(107-115), 37-41.
40. Gao, X. D.; Li, X. M.; Yu, W. D. *J. Inorg. Mater.* **2004**, *19*, 610.
41. Grieve, R. C. *J. Phys. Chem.* **1978**, *82*, 218.
42. Na, J. S.; Kim, D.-H. *et al. Jr. of Electrochemical Soc.* **2002**, *149*(1), C23-27.
43. Benny, J.; Manoj, P. K.; Vaidyan V. K. *Bull. Mater. Sci.* **2005**, *28*(5), 487.
44. Tauber, R. N.; Dumbri, A. C. Caffrey, R. E. *J. Electrochem. Soc. Solid State Sci.* **1971**, *118*, 747.